Estimation of the Force-Interactive Behaviors between Human and Machine Using an Observer-Based Technique

Kuan-Heng Chen and Syh-Shiuh Yeh

Abstract—**This study aims at the development of an observer-based technique for the estimation of force-interactive behaviors between human and machine when the mechanical system executes force tasks. The force-interactive behaviors between human and machine could be similar to that human exert external forces on the mechanical system; thus, the exerted forces affect the execution of the applied axial motion systems in the mechanical system and, therefore, an observer based on the characteristics of a applied axial motion system could be developed to estimate the force-interactive behaviors. In this study, an observer-based technique is developed to estimate the force-interactive behaviors and several topics, such as the modeling error analysis, the filter design consideration, and the observed signal isolation, are also discussed for improving the estimation. Several experiments and motion tests were carried out on an axial motion system so as to illustrate the feasibility of the observer-based technique developed in this study. The experimental results show that the proposed observer-based technique is feasible and could be used to successfully and exactly estimate the force-interactive behaviors between human and machine.**

I. Introduction

External disturbances usually affect the running performances of an axial motion system. Those external disturbances include the load torque caused by Coriolis force, centrifugal force, friction force, and gravity; moreover, the external disturbance includes the force-interactive torque when the mechanical system does the force task [1]. In recent years, the disturbance observer is widely applied to motion control systems for observing external disturbances. Katsura et. al. [1-2] proposed the acceleration based control with the disturbance observer such that the force servoing and the position regulator can be integrated in the acceleration control loop for developing a medical forceps system. Yasui et. al. [3] proposed an adaptive disturbance observer design and applied to engine speed control such that the control system provided accurate and rapid engine speed control under all engine conditions. Liu and Svoboda [4] proposed the integrated controller combined with sliding-mode fuzzy neural network, feedback-error-learning strategy, and nonlinear disturbance observer for improving the precision of the tracking control. Chen [5] proposed a general framework with nonlinear disturbance observer for improving disturbance attenuation ability of a two-link robotic manipulator. Yeh and Hsu [6] proposed a perfectly matched feedback control design with digital disturbance observer for improving the contouring accuracy of multi-axis motion control systems. Kwon and Chung [7] proposed a discrete perturbation observer design in state-space for motion control applications. The effect of the Q-filter on performance and robustness is also discussed in the discrete-time domain. Bertoluzzo et. al. [8] further found that the stability of feedback control system with disturbance observer is closely related to the disturbance observer bandwidth, the current-loop bandwidth, the sampling time and the mismatch in the parameters.

Although excellent performances are usually obtained, some problems still exist on the realization of the disturbance observer [8]. The first problem in implementing the disturbance observer is the need of acceleration signal. In the present research, the acceleration signal is obtained from the double differentiation of the position signal. However, the operation for double differentiation usually generates considerable noise superimposed on the acceleration signal and thus the low-pass filter with narrow bandwidth is required for noise attenuation. The low-pass filter with narrow bandwidth not only slows down the estimation of external disturbances but also deteriorates the transient robustness of control systems. The second problem in implementing the disturbance observer is the need of inverse dynamics. To precisely estimate the external disturbances, the inverse dynamics of the observed plant is applied to the design of disturbance observer. However, the observer using the inverse dynamics induces unstable computation for the discrete-time processing with improper sampling time. Although the digital disturbance observer design with nominal FIR filter proposed

Manuscript received December 8, 2011. This work was supported in part by the National Science Council of the Republic of China under Contract NSC 100-2221-E-027-009 and the Industrial Technology Research Institute, ROC, under project number 9353C72000, which is subcontracted from the Ministry of Economic Affairs, ROC.

K. H. Chen is with the Institute of Mechatronic Engineering, National Taipei University of Technology, Taiwan (phone: +886-2-2771-2171; fax: +886-2-2731-7191; e-mail: khchen@ntut.edu.tw).

S. S. Yeh is with the Department of Mechanical Engineering, National Taipei University of Technology, Taiwan (phone: +886-2-2771-2171; fax: +886-2-2731-7191; e-mail: ssyeh@ntut.edu.tw).

ISBN: 978-988-19251-9-0
ISSN: 2078-0958 (Print); ISSN: 2078-0966 (Online)

by Yeh and Hsu [6] provides stable computation for the discrete-time processing, the performance for estimating external disturbances is limited by the bandwidth of velocity control loop. Considering the realization of disturbance observer, an observer design without acceleration signal and inverse dynamics is needed to exactly estimate external disturbances of an axial motion control system. Murakami et. al. [9] proposed a disturbance observer design with pseudodifferentiator for obtaining the angular acceleration signal. However, the observer design with the first-order low-pass filter can not efficiently isolate the adverse effects caused by noise perturbations.

In some applications, it is not critical for exactly estimating external disturbances and the observation of the effects caused by external disturbances is more important. Because external disturbances usually affect the speed performances of an axial motion system, the observation of speed variations induced by external disturbances is thus instead of the exact estimation of external disturbances for some control applications. In this paper, a disturbance observer is proposed to estimate the speed variations induced by external disturbances. Since the force-interactive behaviors between human and machine are similar to that human exert external disturbances on an axial motion system, it is interesting to estimate the speed variations induced by the force-interactive behaviors. Comparing with the acceleration signal in the design of existing disturbance observers, the speed signal obtained from the single differentiation of position signal is applied to estimate the speed variation of an axial motion control system. Although the operation for single differentiation generates noise superimposed on the speed signal, a conventional low-pass filter is applied to attenuate noise perturbations. The low-pass filter with suitable bandwidth provides good estimation results and maintains the transient robustness of control systems. Moreover, comparing with the existing disturbance observers, the nominal plant without inverse dynamics is applied to design the proposed disturbance observer that provides stable computation for the discrete-time processing. Some specific topics are also discussed in this paper for improving the estimation of the disturbance observer. The design of a low-pass filter is concerned for reducing the adverse effects caused by modeling errors and measurement noises that usually deteriorate the estimation of an observer. Because the disturbance observer obverses the mixed phenomena induced by load torque and force-interactive torque, a disturbance isolation method is discussed to identify the source of disturbances such that observer can estimate speed variations caused by the force-interactive behaviors between human and machine.

II. Design of Disturbance Observer

Considering the disturbance observer as shown in Fig. 1. T is the sampling time. $u^*(t)$ is the sampled driving force from digital controller and $U^*(s)$ is the corresponding transformation in frequency domain. $\tau(t)$ is the torque command for driving servo systems. It's also the output signal of Zero-order-hold filter $H(s)$ with input signal $u^*(t)$. $T(s)$ is the corresponding transformation in frequency domain. $\tau(t)$ is the torque command for driving servo systems. It's also the output signal of Zero-order-hold filter with input $u^*(t)$. $T(s)$ is the corresponding transformation in frequency domain. $\tau_d(t)$ is the torque disturbance from environment. $\tau_d^*(t)$ is the sampled torque disturbance and $T_d{}^*(s)$ is the corresponding transformation in frequency domain. $w(t)$ is the rotating speed of servo motor and $W(s)$ is the corresponding transformation in frequency domain. $\theta(t)$ is the angular position of servo motor. $\delta^*(t)$ is the high frequency noise signal and $\Delta^*(s)$ is the corresponding transformation in frequency domain. $v^*(t)$ is the sampled rotating speed of servo motor and $V^*(s)$ is the corresponding transformation in frequency domain. The signal contains the high frequency noise signal $\delta^*(t)$. $d^*(t)$ is the estimated disturbance signal in discrete time domain and $D^*(s)$ is the corresponding transformation in frequency domain. $\hat{d}^*(t)$ is the output signal from digital low-pass filter $LPF(z^{-1})$ with estimated disturbance $d^*(t)$ as the input signal. $G(s)$ is the referred dynamic system. $H(s)$ is the zero-order-hold (Z.O.H) filter. $LPF(z^{-1})$ is the applied low-pass filter.

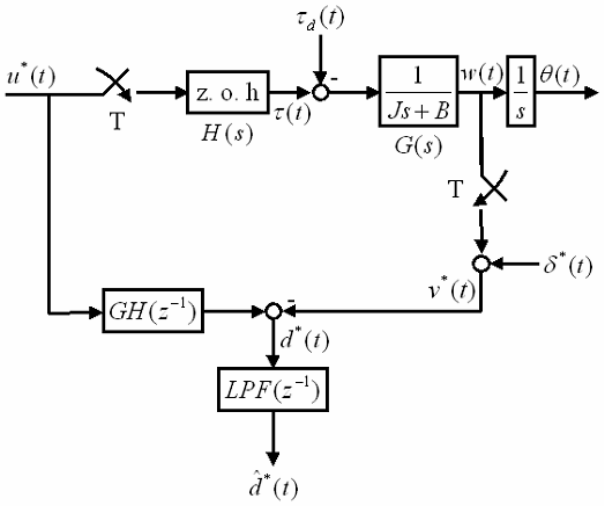

Fig. 1. The proposed discrete-time disturbance observer.

Since,

$$T(s) = U^*(s)H(s)$$

and

$$W(s) = G(s)[T(s) - T_d(s)] = G(s)H(s)U^*(s) - G(s)T_d(s)$$

The sampled rotating speed of servo motor without noise

perturbation is obtained as

$$W^*(s) = L\{w^*(t)\} = GH^*(s)U^*(s) - GT_d{}^*(s)$$

and the sampled rotating speed of servo motor is thus obtained as

$$V^*(s) = W^*(s) + \Delta^*(s) = GH^*(s)U^*(s) - GT_d{}^*(s) + \Delta^*(s)$$

Therefore, the estimated disturbance signal is derived as

$$D^*(s) = GH^*(s)U^*(s) - V^*(s) = GT_d{}^*(s) - \Delta^*(s)$$

By applying the definition of the Z-transformation, the estimated disturbance signal is represented as

$$D(z^{-1}) = GT_d(z^{-1}) - \Delta(z^{-1}) \quad (1)$$

Eq. (1) denotes the estimated disturbance signal $d^*(t)$ contains the filtered disturbance $GT_d(z^{-1})$ and high frequency noise signal $\delta^*(t)$. To degrade the adverse effects caused by high frequency noise signal $\delta^*(t)$, the low-pass filter is applied to the estimated disturbance signal $d^*(t)$. The filtered disturbance signal $\hat{d}^*(t)$ is thus obtained as

$$\hat{D}(z^{-1}) = LPF(z^{-1})GT_d(z^{-1}) - LPF(z^{-1})\Delta(z^{-1}) \quad (2)$$

where $\hat{D}(z^{-1})$ is the Z-transformation of the output signal $\hat{d}^*(t)$. For low-pass filter designed with suitable cutoff frequency, Eq. (2) can be rewritten as

$$\hat{D}(z^{-1}) \cong LPF(z^{-1})GT_d(z^{-1}) \quad (3)$$

Eq. (3) denotes that the torque disturbance from environment could be estimated from observed signal $\hat{d}^*(t)$. Clearly, Eq. (3) denotes that the observed value $\hat{d}^*(t)$ is the filtered response of external disturbance $\tau_d(t)$; moreover, the observed value $\hat{d}^*(t)$ responds to the fluctuation of rotating speed induced by external disturbance $\tau_d(t)$. Although the speed variation induced by external disturbances is observed by applying the observer as shown in Fig. 1, some topics must be further discussed for improving the performance of observer.

III. The Post Processing Unit

As shown in Fig. 1, by replacing filter $GH(z^{-1})$ with nominal filter $G_nH(z^{-1})$, the estimated disturbance signal $D^*(s)$ is obtained as

$$D^*(s) = G_nH^*(s)U^*(s) - V^*(s)$$

where, $G_n(s)$ is the nominal model of $G(s)$. It's usually obtained by regular system identification method [10]. Because the sampled rotating speed of servo motor is derived as

$$V^*(s) = W^*(s) + \Delta^*(s) = GH^*(s)U^*(s) - GT_d{}^*(s) + \Delta^*(s)$$

The estimated disturbance signal $D^*(s)$ is rewritten as

$$D^*(s) = \left[G_nH^*(s) - GH^*(s)\right]U^*(s) + GT_d{}^*(s) - \Delta^*(s)$$

or

$$D(z^{-1}) = \left[G_nH(z^{-1}) - GH(z^{-1})\right]U(z^{-1}) + GT_d(z^{-1}) - \Delta(z^{-1}) \quad (4)$$

Eq. (4) represents the estimated disturbance signal in discrete-frequency domain. As shown in Eq. (4), Eq. (1) is obtained when the nominal model $G_n(s)$ is exactly the same as plant $G(s)$. By applying the low-pass filter as shown in Fig. 1, the observed value $\hat{D}(z^{-1})$ is obtained as

$$\hat{D}(z^{-1}) = LPF(z^{-1})\left[G_nH(z^{-1}) - GH(z^{-1})\right]U(z^{-1}) + LPF(z^{-1})GT_d(z^{-1}) - LPF(z^{-1})\Delta(z^{-1}) \quad (5)$$

For low-pass filter designed with suitable cutoff frequency, Eq. (5) can be rewritten as

$$\hat{D}(z^{-1}) \cong LPF(z^{-1})\left[G_nH(z^{-1}) - GH(z^{-1})\right]U(z^{-1}) + LPF(z^{-1})GT_d(z^{-1}) \quad (6)$$

Define the perturbation function $P_e(z^{-1})$ as

$$P_e(z^{-1}) = LPF(z^{-1})\left[G_nH(z^{-1}) - GH(z^{-1})\right] \quad (7)$$

Eq. (6) can be further rewritten as

$$\hat{D}(z^{-1}) \cong P_e(z^{-1})U(z^{-1}) + LPF(z^{-1})GT_d(z^{-1}) \quad (8)$$

Therefore, a precise model $G_n(s)$ is required for degrading the adverse effects caused by modeling error.

The observer as shown in Fig. 1 observes the disturbance induced by external disturbances include the force-interactive torque when the mechanical system does the force task and the load torque caused by Coriolis force, centrifugal force, friction force, and gravity force. Similar to the load torque compensation proposed by Katsura [1] and Murakami [9], the speed variation caused by specific load torque is identified by compensating the speed variation caused by other load torque. For instance, for estimating the speed variation caused by force-interactive torque, the speed variation caused by load torque must be compensated.

As shown in Fig. 1, one of the main concern in designing the low-pass filter $LPF(z^{-1})$ is for reducing the adverse effects caused by measurement noise. However, when the frequency responses of modeling error $\left[G_nH(z^{-1}) - GH(z^{-1})\right]$ are in higher frequency range, the low-pass filter design with suitable bandwidth reduces the perturbation $P_e(z^{-1})U(z^{-1})$ caused by modeling error. Thus, in this paper, the design of low-pass filter $LPF(z^{-1})$ is for reducing the adverse effects caused by measurement noise and modeling error.

IV. Experimental Results: Axial Mechanical System

The experimental setup for the present study is shown in Fig. 2. The applied motion control system consists of a personal computer, a DSP-based motion control card, and an axial mechanical system. The personal computer and DSP-based motion control card generated control commands

ISBN: 978-988-19251-9-0
ISSN: 2078-0958 (Print); ISSN: 2078-0966 (Online)

and recorded signals, including: the input commands for controllers, position outputs, and the driving forces for AC servo drivers. The DSP-based motion control card has built-in a high-performance TI TMS320C32 digital signal processor (DSP), which is capable of implementing some functions at a sampling period of 1 ms. The axial mechanical system is composed of a Panasonic AC servo motor, a gear set, and a handler. The mechanical system can perform a force task when operator manually operates the handler that is built at the top of gear set. The experimental setup is used for testing the proposed disturbance observer.

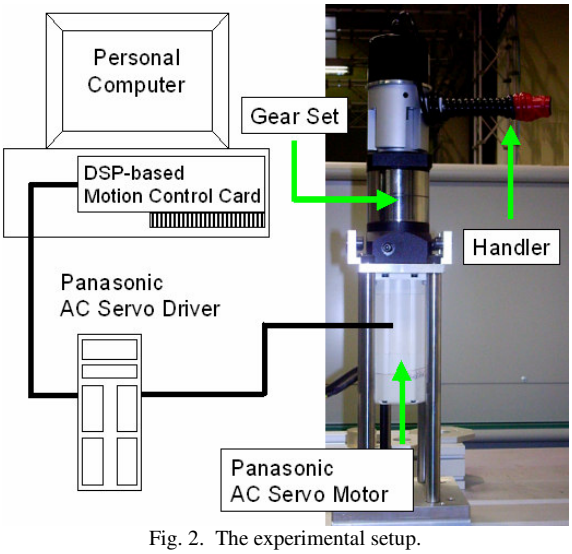

Fig. 2. The experimental setup.

The torque equation of the applied axial mechanical system is written as

$$J_m\ddot{\theta}_m + B_m\dot{\theta}_m = T_m$$

where θ_m is the angular displacement, $\dot{\theta}_m$ is the angular velocity, and $\ddot{\theta}_m$ is the angular acceleration. J_m denotes the equivalent inertia of an axial mechanical system. B_m denotes the lumped viscous-friction coefficient. T_m is the applied torque and R is the gear ratio. By applying the identification algorithm [10], the system parameters (J_m, B_m) are obtained as

$$J_m = 0.000031369\,;\ B_m = 0.00039\,;\ R = 0.04$$

For testing the identified parameters, the step responses with different step input commands are compared in this paper. As shown in Fig. 3, the testing results show that the identified parameters are acceptable for designing the disturbance observer.

Before designing the low-pass filter $LPF(z^{-1})$, frequency analysis of modeling error is performed for obtaining more design information in frequency domain. The frequency responses of modeling error before applying low-pass filter is shown in Fig. 4. The modeling error is enlarged after 3Hz. Therefore, to reduce the adverse effects caused by modeling error, the low-pass filter is designed with bandwidth less than 3Hz.

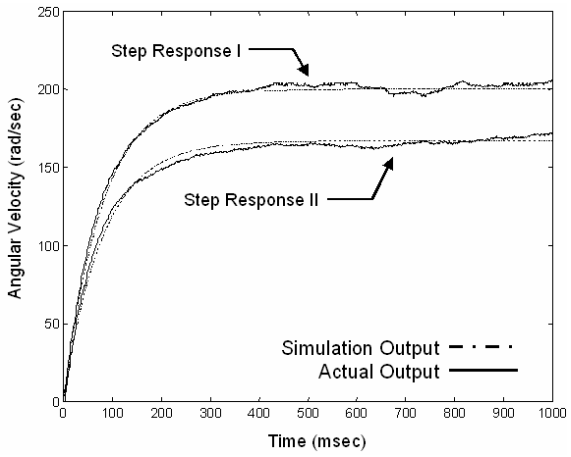

Fig. 3. Step responses of the axial motion system.

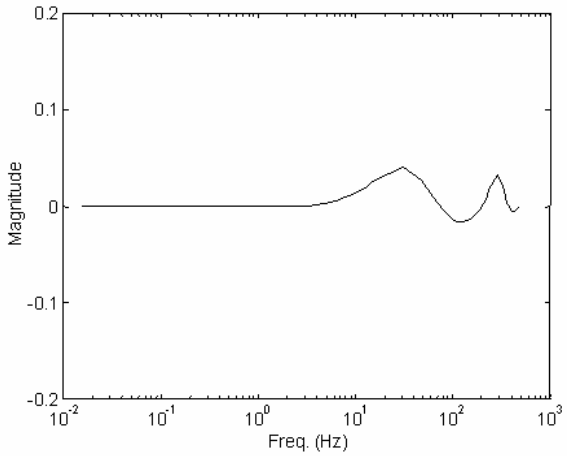

Fig. 4. The frequency response of modeling error.

The frequency analysis of measurement noise is performed before designing the low-pass filter $LPF(z^{-1})$. Fig. 5 shows the frequency responses of measurement noise. Obviously, the low-pass filter with bandwidth less than 4Hz is required for reducing the adverse effects caused by measurement noise.

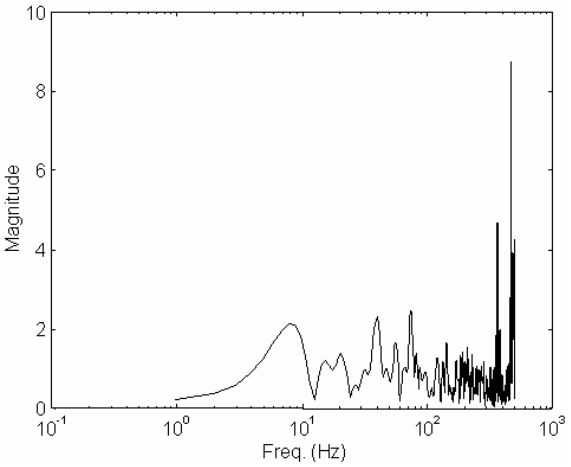

Fig. 5. The frequency response of measurement noise.

Therefore, according to the frequency analysis of modeling

ISBN: 978-988-19251-9-0
ISSN: 2078-0958 (Print); ISSN: 2078-0966 (Online)

error and measurement noise, a 4th-order low-pass filter $LPF(z^{-1})$ is designed as

$$LPF(z^{-1}) = \frac{\begin{pmatrix} 0.0770 + 0.3080z^{-1} + 0.4619z^{-2} \\ + 0.3080z^{-3} + 0.0770z^{-4} \end{pmatrix} \times 10^{-7}}{1 - 3.9507z^{-1} + 5.8534z^{-2} - 3.8546z^{-3} + 0.9519z^{-4}}$$

For testing the performance of disturbance observer, a force task is performed on the axial mechanical system as shown in Fig. 2. Fig. 6 and Fig. 7 show the experimental results of the axial motion control system with different control laws. The force-interactive torque is applied to the mechanical system by swing the handler. Fig. 6 shows the experimental result of the torque controlled axial motion system. The observer quickly responses the speed variation caused by force-interactive torque. Fig. 7 shows the experimental result of the position controlled axial motion system. The damping responses are observed when the handler is released after swing operation.

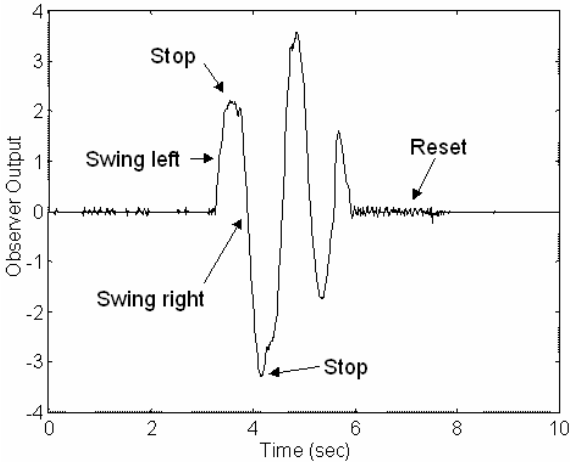

Fig. 6. The disturbance caused by force-interactive torque.

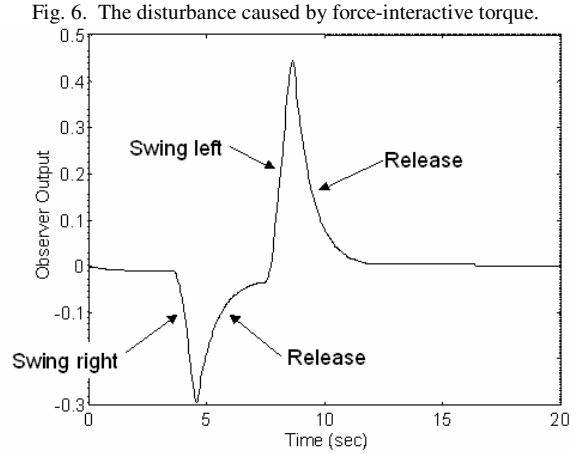

Fig. 7. The disturbance observed under position control.

V. Experimental Results: Mobile Robot

In order to demonstrate the design and application of the observer developed in this study, a mobile robot is developed with compliant motion control design. Fig. 8 shows the design of the mobile robot. The mobile robot consists of two main parts: a humanoid body and a two-wheeled mobile platform. The two-wheeled mobile platform is equipped with two tracked drive-wheels so that it can move successfully on uneven surfaces. The humanoid body with eight joints is developed to perform force-interactive tasks with human. The mobile robot uses ten AI motors [11] developed by MEGAROBOTICS Company so that the mobile robot can be controlled through the use of serial communication. The DSP-based control card with a high-performance MicroChip DSPic30F4011 DSP is used as the interface for sending motion commands to and for receiving feedback signals from the applied AI motors with a sampling period of 0.05 s.

Fig. 8. Photograph of the mobile robot.

In this experiment, the compliant motion control design is developed and implemented on the mobile robot; thus, the mobile robot can move and perform motions according to the force-interactive behaviors between human and the humanoid body of the mobile robot. In order to estimate the force-interactive behaviors, the disturbance observer developed in this study is applied to each AI motor and the interactive forces corresponding to the force-interactive behaviors can be estimated by referring to the observed signals and the kinematic analysis of the mobile robot. Then, based on the estimated interactive forces, the mobile robot performs compliant motions to respond to the force-interactive behaviors. Fig. 9 shows the estimated interactive forces when the mobile robot suffers different force-interactive behaviors. Fig. 9(a) and Fig. 9(b) respectively show the estimated interactive forces when the human pushes and pulls the chest and the right hand of the humanoid body. Fig. 10 shows the compliant behavior of the mobile robot when the human pushes and pulls the chest of the humanoid body. Obviously, the humanoid body falls down and the mobile robot moves forward when the human pulls the chest; the humanoid body rises up and the mobile robot moves backward when the human pushes the chest. Therefore, the experimental results demonstrate the feasibility and the application of the observer design developed in this study.

ISBN: 978-988-19251-9-0
ISSN: 2078-0958 (Print); ISSN: 2078-0966 (Online)

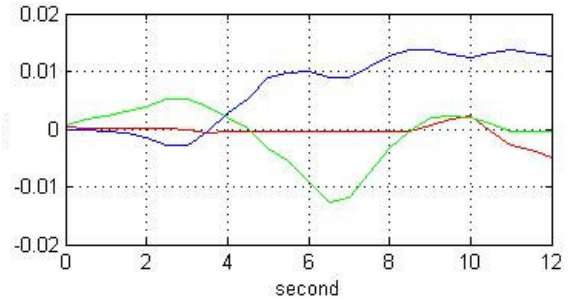

(a) Force-interactive behavior I (chest-operation)

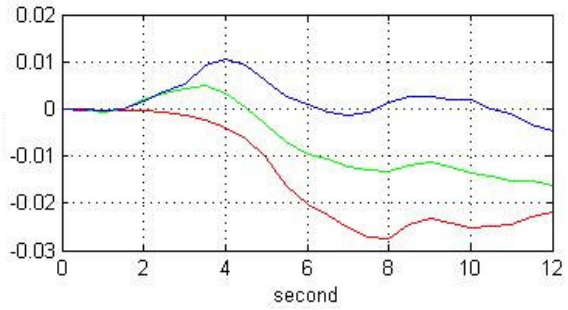

(b) Force-interactive behavior II (hand-operation)

Fig. 9. The estimated interactive forces corresponding to different force-interactive behaviors.

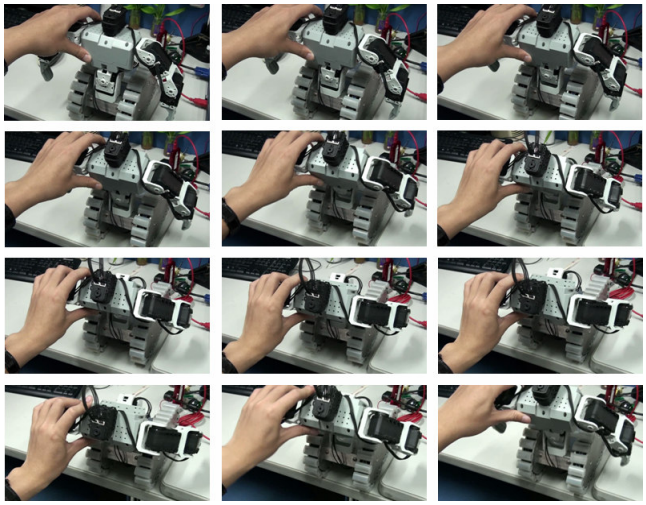

Fig. 10. Compliant behaviors of the mobile robot.

VI. Conclusion

A disturbance observer for estimating the speed variations caused by the force-interactive behaviors between human and machine is proposed in this paper. Comparing with the existing approaches, the proposed observer design is less sensitive to measurement noises and provides stable computation for the discrete-time processing. Moreover, the post-processing unit applied to further process the observed signal is proposed to reduce the adverse effects caused by modeling errors and to identify the speed variation caused by specific load torque. In this paper, the specific load torque implies the specific force-interactive behavior between human and machine. The design of a low-pass filter is also discussed for reducing the adverse effects caused by modeling errors and measurement noises that usually deteriorate the estimation of an observer. Finally, some experimental tests are given to evaluate the performance of the proposed observer design. The experimental results show that the proposed approach exactly responses the speed variations caused by force-interactive behaviors.

References

[1] S. Katsura, Y. Matsumoto, and K. Ohnishi, “Realization of "law of action and reaction" by multilateral control,” IEEE Transactions on Industrial Electronics, vol. 52, no. 5, pp. 1196-1205, October, 2005.

[2] S. Katsura, W. Iida, and K. Ohnishi, “Medical mechatronics - An application to haptic forceps,” Annual Reviews in Control, vol. 29, no. 2, pp. 237-245, 2005.

[3] Y. Yasui, K. Shimojo, M. Saito, and H. Tamagawa, “Accurate engine speed control using adaptive disturbance observer,” Review of Automotive Engineering, vol. 26, no. 2, pp. 137-141, April, 2005.

[4] Z. L. Liu and J. Svoboda, “A new control scheme for nonlinear systems with disturbances,” IEEE Transactions on Control Systems Technology, vol. 14, no. 1, pp. 176-181, January, 2006.

[5] W. H. Chen, “Disturbance observer based control for nonlinear systems,” IEEE/ASME Transactions on Mechatronics, vol. 9, no. 4, pp. 706-710, December, 2004.

[6] S. S. Yeh and P. L. Hsu, “Perfectly Matched Feedback Control and Its Integrated Design for Multi-Axis Motion Systems,” ASME Journal of Dynamic Systems, Measurement and Control, vol. 126, no. 3, pp. 547-557, 2004.

[7] S. J. Kwon and W, K, Chung, “A discrete-time design and analysis of perturbation observer for motion control applications,” IEEE Transactions on Control Systems Technology, vol. 11, no. 3, pp. 399-407, May, 2003.

[8] M. Bertoluzzo, G. S. Buja, and E. Stampacchia, “Performance analysis of a high-bandwidth torque disturbance compensator,” IEEE/ASME Transactions on Mechatronics, vol. 9, no. 4, pp. 653-660, December, 2004.

[9] T. Murakami, F. Yu, and K. Ohnishi, “Torque Sensorless Control in Multidegree-of-Freedom Manipulator,” IEEE Transactions on Industrial Electronics, vol. 40, no. 2, pp. 259-265, April, 1993.

[10] Söderström, T., and Stoica, P., (1989), System Identification, Prentice Hall.

[11] MEGAROBOTICS Co., (2002), AI Motor-701 Manual ver. 1.02.

ISBN: 978-988-19251-9-0
ISSN: 2078-0958 (Print); ISSN: 2078-0966 (Online)